

# Upgrade of the ATLAS MDT Readout and Trigger for the HL-LHC

---

**Robert Richter**\* †

*Max-Planck-Institute for Physics, Munich*

*E-mail:* [Robert.Richter@cern.ch](mailto:Robert.Richter@cern.ch)

The luminosity increase at the LHC in Phase-II calls for an in-depth redesign of the Monitored Drift Tube (MDT) chamber readout. One reason for this is the high rate of primary detector signals which requires increased readout bandwidth all along the data path. The second reason is due to a new concept for the formation of the Level-1 muon trigger (L1), which aims to improve the selectivity for muons with high transverse momentum ( $p_T$ ). While in the present system the L1 trigger is exclusively based on specialized trigger chambers (RPC in the barrel, TGC in the endcap), which deliver tracking information with very limited accuracy, the L1 trigger will, in Phase-II, also consider tracking information from the MDT: the time resolution of the trigger chambers, able to tag the beam crossing (BX), will be combined with the high spatial accuracy of the MDT.

In the new L1 trigger scheme, the selection of MDT hits corresponding to a given BX, will be based on a Region of Interest (RoI) provided by the trigger chambers. Considering only MDT hits in the RoI will result in a large reduction of the relevant data volume. The selected MDT hits will be tested for consistency with the track direction, as defined by the RoI. If confirmed, the MDT hits are used for a better  $p_T$  definition.

The rate of background hits from  $\gamma$  and neutron conversions is several orders of magnitude higher than the one from muon hits. The selection of muons against this background ("hit extraction") requires high-speed processing power, capable to supply the relevant information to the Muon Central Trigger Processor (MUCTPI) inside the latency of 10  $\mu$ s.

*Topical Workshop on Electronics for Particle Physics TWEPP2019*

*2-6 September 2019*

*Santiago de Compostela - Spain*

---

\*Speaker.

†On behalf of the ATLAS Collaboration.

## 1. Introduction

The increase of luminosity at the LHC in Phase-II by a factor 7 w.r.t. the original design luminosity of  $10^{34} \text{ cm}^{-2}\text{s}^{-1}$  represents a big challenge for the readout of all ATLAS subdetectors as the readout bandwidth must be increased by nearly an order of magnitude.

Due to the necessity to include MDT data in the L1 trigger, the present readout mode, where only MDT hits from *triggered* beam crossings are retained, had to be abandoned in favour of a mode where *all* hits recorded in the MDT tubes are transferred to the L1 trigger logics and to the back-end electronics. This allows to use the high spatial accuracy of the MDT in the L1 trigger decision, opening a new opportunity to improve trigger selectivity for high- $p_T$  tracks.

Details of the new Trigger and Data Acquisition architecture (TDAQ) and of the Muon Spectrometer readout in Phase-II are given in Ref. [1] [2] and [3] [4], respectively.

## 2. Selectivity of the Muon Trigger for high- $p_T$ Muons

The total inelastic cross section in p-p collisions at LHC energies is about 88 mb, while the cross section for muons reaching the muon detector, i.e. muons with  $p_T > 4 \text{ GeV}$ , is only a few  $\mu\text{b}$  - roughly 4 orders of magnitude less. Among these muons, the fraction of high- $p_T$  muons, i.e. with a transverse momentum above 20 GeV, is only 40 nb.

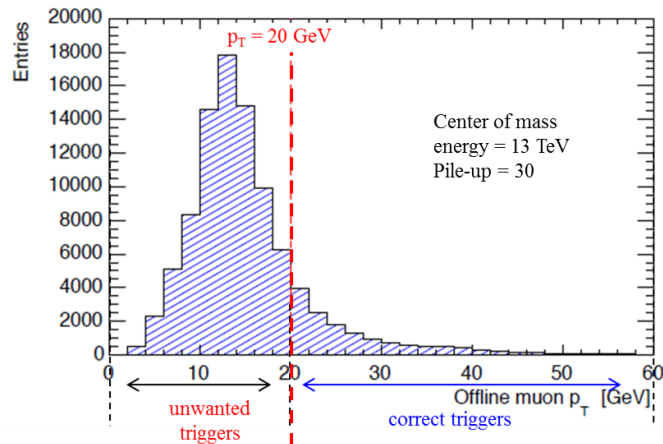


**Figure 1:** Off-line distribution of muons identified by the L1 trigger at a  $p_T$  threshold of 20 GeV [1]

Muons with high- $p_T$  are frequently decay products of heavy particles like Z, W, tt or exotics, and thus belong to a class of interesting physics event signatures. Therefore, high- $p_T$  muons need to be identified at an early stage, rejecting those below the 20 GeV threshold, which are mostly coming from decays of heavy quarks or  $\pi/K$  in hadronic showers.

The selectivity of the present muon trigger was tested when the "real"  $p_T$  of triggered high- $p_T$  tracks was reconstructed off-line. In the off-line analysis, information from MDT chambers, from the Inner Detector and from accurate magnetic field maps along the trajectory are available for a precise measurement of the muon track. Fig. 1 shows that the large majority of muons triggered at Level-1 was, in fact, below the critical threshold.

The reason for this lack of accuracy at the trigger level is the limited spatial resolution of the trigger chambers, RPC in the barrel and TGC in the endcap. The  $p_T$  measurement of both chamber types is based on readout strips, perpendicular to the bending plane, with strip widths of 3–6 cm. As the sagitta of a 20 GeV track is of the order of 1 cm, the actual  $p_T$  can only be determined in an approximate way, insufficient for a sharp  $p_T$  threshold.

### 3. Using MDT Coordinates for better $p_T$ -selection

In the Muon Spectrometer each trigger chamber is matched to a MDT precision chamber, which measures the track coordinates with an accuracy of about 0.1 mm. In the barrel, e.g., three layers of MDT and RPC are arranged in projective towers (see ref. [3]), such that most tracks with small curvature ("nearly straight") are enclosed inside *one* tower, simplifying the determination of  $p_T$ . Due to the combination of MDT and trigger chamber measurements at the L1 trigger level, foreseen in Phase-II, a more accurate  $p_T$  determination and a considerable reduction of sub-threshold triggers will be achieved.

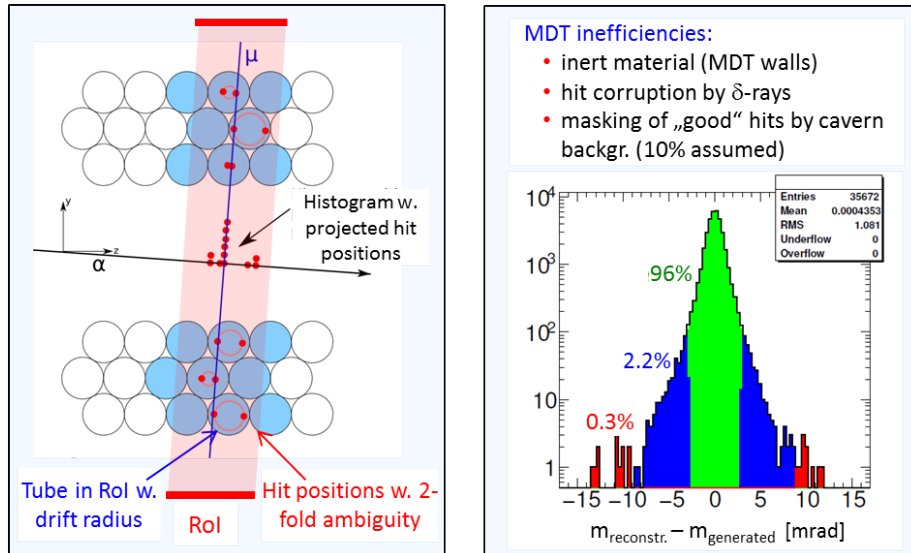


**Figure 2:** The histogramming method (left) and the resulting efficiency (right).

This requires an additional processing step in the generation of the L1 trigger, whereby the trigger chambers will be used to indicate beam crossing time (BX) and the approximate location of a trigger candidate, called Region of Interest (RoI), while the MDT hits are used for an accurate definition of the track coordinates. First, a track segment in each MDT chamber is derived from the hits in the RoI. Subsequently, the track segments of three MDT/RPC pairs are combined, resulting in an accurate  $p_T$ . This way, most sub-threshold trigger candidates can be suppressed.

Fig. 2 (left) illustrates the matching method between the RoI and the MDT hit candidates. A histogram is filled by projecting all MDT hits onto a plane perpendicular to the direction of the RoI. The maximum in the histogram denotes the most likely candidate for the muon track segment in the given RoI. This method automatically discards fake hits caused by the left-right ambiguity of MDT measurements as well as uncorrelated hits from  $n/\gamma$ -conversion, which in some regions of

the detector may reach occupancies of up to 10 %. Once the relevant MDT hits identified, a  $\chi^2$ -test is performed for this track segment. The three track segments inside a trigger tower are finally combined to determine the track curvature and  $p_T$ .

The right side of Fig. 2 shows the result of a simulation which takes into account the most important deteriorating effects for track identification, like  $\delta$ -electrons, inefficiencies due to hits from  $n/\gamma$  conversion or due to tracks passing through inert material. The distribution is described by a gaussian with a small admixture of non-gaussian tails. It shows that about 96 % of the track candidates are *correctly* identified, which we define as the difference of slopes between the simulated and reconstructed track to be  $\leq 3\sigma$ .

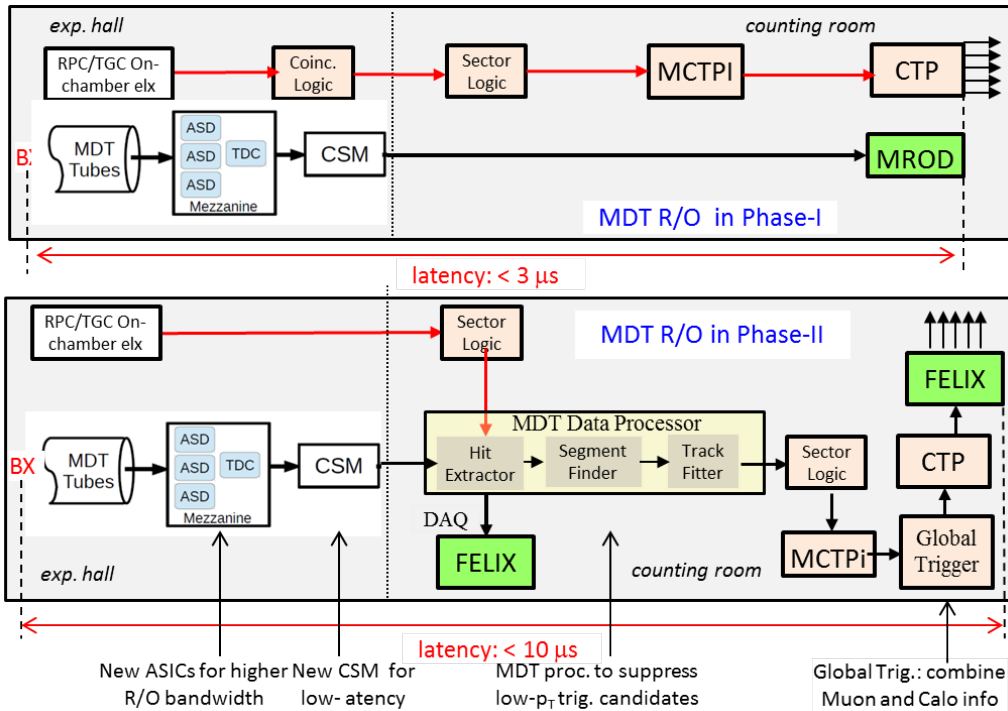


**Figure 3:** Architecture of the present (top) and future (bottom) readout of the Muon system.

#### 4. Technical Implementation

Fig. 3 shows the present and future readout architecture. In the present scheme (top), MDT and RPC/TGC data follow an independent readout path during the L1 latency. In Phase-II (bottom), the MDT Data Processor collects data from both data streams and only allows L1 trigger candidates with  $p_T$  above 20 GeV, as confirmed by MDT tracking, to be forwarded to the MUTCPI and further to the Global Trigger.

The left part of the figure also shows that the structure of the on-chamber readout of the MDT is retained in Phase-II. Due to the requirement of higher readout bandwidth and trigger rate, however, new ASICs had to be developed. The first element in the readout chain, the Amplifier-Shaper-Discriminator (ASD) showed better performance than the legacy one (Agilent 500 nm), w.r.t. peaking time, threshold dispersion among the 8 channels and noise. The mismatch of analog

parameters (gain, peaking time) among the 8 channels and between different chips was at the level of 1–2%. The yield of good chips, obtained in the engineering run, is above 98%.

The TDC has been redesigned for faster readout towards the next stage and for reduced latency. The latter is achieved by assigning a separate derandomizing buffer to *each* channel, while there was only one common buffer for all 24 channels in the legacy device. Prototype TDC chips confirm the simulated performance. A second prototype with only minor modifications, serving as production prototype, has already been submitted.

The CSM design (Chamber Service Module) is based on the lpGBT readout scheme and does not contain radiation sensitive components like FPGAs. Table 1 shows the main components in the MDT readout chain, where new hardware will be installed.

Component	Function	#	Technology	Main Perf. Criteria
ASD	8-ch ASD	60 k	GF 130 nm	Thresh. dispersion, ENC
TDC	serv. 3 ASDs	20 k	TSCM 130 nm	Transmission rate, latency
CSM	serv. 18 TDCs	1.5 k	lpGBT	Latency, data integrity
Trig. proc.	serv. 3 CSMs	500	FPGA, Zynq	Latency, processor speed

**Table 1:** New components of the MDT readout

## 5. Filtering of the Muon Trigger at the MUCTPI and Global Trigger

While each Sector Logic (SL) module controls only a small angular range in  $\eta$  and  $\phi$ , the MUCTPI, collecting the information of all SL units, may discover more than one muon trigger candidate in barrel or endcap. The presence of two muons in a given BX ("di-muon events"), is often caused by decays of heavy vector mesons like  $\Phi$ ,  $J/\Psi$  and  $\Upsilon$ . As  $\mu\mu$ -decays of particles with known mass are instrumental for detector calibration, the MUCTPI accepts di-muon triggers, if the  $p_T$  of at least one of them is above a threshold (e.g. 10 GeV), lower than the single muon threshold of 20 GeV. Selecting di-muon triggers, the MUCTPI has to suppress fake candidates, caused by double counting due to the overlap in  $\Phi$  of adjacent trigger chambers.

At the next level of trigger refinement, the Global Trigger, muon and calorimeter trigger candidates are compared w.r.t. their relative angle. If the angular separation between a jet and a muon is below a critical value, the L1 trigger will be suppressed, as the muon was, most likely, produced by a heavy quark decay or by an in-flight decay of a shower particle ( $\pi/K$ ).

At the level of the CTP, prescaling may be implemented, if required by the trigger menu. The final L1 decision is sent to FELIX, from where the trigger is broadcast to all detector frontends.

## 6. Efficiency of the L1 Muon trigger in Phase-II

Fig. 4 shows the expected trigger rates for single muons in Phase-II as a function of  $\eta$ . The top distribution (white), corresponds to the present L1 architecture. The middle distribution (blue) shows the expected rates due to the MDT trigger processor. The bottom distribution (green) shows the rates after full off-line reconstruction of the muon  $p_T$ . In the middle distribution, one observes two peaks of false triggers at the overlap region between barrel and endcap ( $|\eta| \simeq 1.7$ ).

In this region, muon tracks are passing through the magnetic fields of both, barrel and endcap toroids, providing an inhomogeneous local magnetic field, which results in considerable uncertainties for  $p_T$ . Off-line analysis, in contrast, has detailed magnetic field maps at its disposition, and can, equally important, match muon spectrometer tracks with the corresponding track in the Inner Detector.

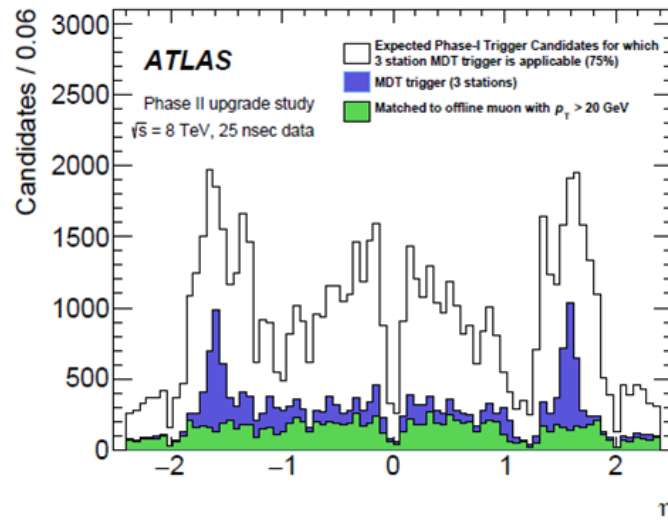


**Figure 4:** The efficiency of the L1 trigger compared to the off-line analysis [1].

## 7. Conclusions

The combination of trigger and precision chamber information will reduce the L1 muon trigger rate by about a factor of four. From the 1 MHz L1 rate in Phase-II, only about 38 kHz will be used by the single and about 10 kHz by the di-muon trigger, while in Phase-I these numbers were 15 and 5 kHz, only a factor two higher than in Phase-I, while the luminosity will increase by a factor of about 7.

The new readout architecture requires a complete replacement of the readout chains of MDT and trigger chambers as well as the installation of new processors for the formation of the combined trigger. Tests of fully functional prototypes of all components are presently under way. Critical performance figures are: sustained data rates, bit error rates, latency, power requirements and cost.

## References

- [1] The ATLAS Collaboration, *TDR for the Phase-II Upgrade of Trigger and DAQ*, ATL-COM-DAQ-2017-185, Dec. 2017
- [2] The ATLAS Collaboration, *TDR for the Phase-II Upgrade of the ATLAS Muon Spectrometer*, CERN-LHCC-2017-017, ATLAS-TDR-026-2017
- [3] The ATLAS Collaboration, *The ATLAS Experiment at the CERN Large Hadron Collider*, JINST **3** S08003 (2008)
- [4] Y. Arai et al., *ATLAS Muon Drift Tube Electronics*, JINST **3** P09001 (2008)